



HAL
open science

Energy band alignment between $\text{Pb}(\text{Zr},\text{Ti})\text{O}_3$ and high and low work function conducting oxides from hole to electron injection

F Chen, R Schafranek, S Li, W B Wu, A Klein

► **To cite this version:**

F Chen, R Schafranek, S Li, W B Wu, A Klein. Energy band alignment between $\text{Pb}(\text{Zr},\text{Ti})\text{O}_3$ and high and low work function conducting oxides from hole to electron injection. *Journal of Physics D: Applied Physics*, 2010, 43 (29), pp.295301. 10.1088/0022-3727/43/29/295301 . hal-00597826

HAL Id: hal-00597826

<https://hal.science/hal-00597826>

Submitted on 2 Jun 2011

HAL is a multi-disciplinary open access archive for the deposit and dissemination of scientific research documents, whether they are published or not. The documents may come from teaching and research institutions in France or abroad, or from public or private research centers.

L'archive ouverte pluridisciplinaire **HAL**, est destinée au dépôt et à la diffusion de documents scientifiques de niveau recherche, publiés ou non, émanant des établissements d'enseignement et de recherche français ou étrangers, des laboratoires publics ou privés.

Energy band alignment between $\text{Pb}(\text{Zr,Ti})\text{O}_3$ and high and low work function conducting oxides - from hole to electron injection

F. Chen †, R. Schafranek †, S.Li†, W. B. Wu ‡, A. Klein †

† Technische Universität Darmstadt, Institute of Materials Science, Petersenstraße 23, D-64287 Darmstadt, Germany

‡ Hefei National Laboratory for Physical Sciences at the Microscale, University of Science and Technology of China, Hefei 230026, China

E-mail: rschafranek@surface.tu-darmstadt.de (R. Schafranek)

Abstract. The interface formation between $\text{Pb}(\text{Zr,Ti})\text{O}_3$ (PZT) and RuO_2 and between PZT and $\text{In}_2\text{O}_3:\text{Sn}$ (ITO), respectively was characterised using *in-situ* X-ray photoelectron spectroscopy (XPS). No interface reaction was observed for the interfaces studied. The Fermi level position at the interface (Schottky barrier height) is strongly different for the two electrode materials. A Fermi level position of 1.0 ± 0.1 eV above the valence band maximum (VBM) is observed for the contact between PZT and the high work function oxide RuO_2 . For the contact between PZT and the low work function oxide ITO a Fermi level position of 2.1 ± 0.2 eV above the VBM is found.

PACS numbers: 73.30.+y 79.60.Jv 77.84.Cg

1. Introduction

Lead zirconate titanate ($Pb(Zr,Ti)O_3$, PZT) is one of the most commonly used ferroelectric materials applied e.g. in thin film form as capacitors in non-volatile memories [1] as well as in bulk form in piezoelectric sensors and actuators [2]. Electrical fatigue (reduction of the polarization with increasing switching cycles) limits the reliability of these devices and is therefore a crucial issue [1, 3, 4]. In the case of thin PZT films, leakage current and fatigue properties are dependent on the electrode material used [1, 5, 6, 7, 8]. While for Pt electrodes a pronounced fatigue is observed, the use of oxidic electrodes as RuO_2 , $LaSr_{0.5}Co_{0.5}O_3$ or $SrRuO_3$ leads to less fatigue. The observed fatigue of Pt/PZT/Pt capacitors may be linked to the injection of charge carriers (a) inhibiting the formation of opposite domains or (b) leading to an effective low relative permittivity layer ([3] and references within). An alternative explanation for the fatigue improvement observed with oxide electrodes is the redistribution and pile-up of oxygen vacancies at the ferroelectric/metal interface with increasing switching cycles, thus hindering the switching process. Oxidic electrodes are supposed to absorb oxygen vacancies [9, 10], leading to less fatigue. However, polarisation fatigue was also observed for n-type conductive electrodes like $In_2O_3:Sn$ (ITO) [11, 12] and $SrSnO_3:La$ [13, 14]. This points to the fact that the PZT polarisation fatigue is more related to the electronic interface properties, which is also supported by the results of Du and Chen [15]. They observed a stronger fatigue improvement using a p-type Si barrier as compared to a n-type Si barrier. Therefore the injection of electrons, rather than holes, might be related to PZT fatigue.

Although, device properties as fatigue are evidently linked to the interface properties, the interface between PZT and different electrode materials was scarcely investigated. In bulk form PZT shows p-type conductivity due to Pb vacancies [16, 17]. However, there has been a dispute in literature whether the current transport in PZT thin films is dominated by electrons or holes [1, 18]. For electronic devices the interface properties play a crucial role as the choice of contact material determines the Fermi level position in the PZT at the interface, which corresponds to the zero field Schottky barrier height for electrons or holes, respectively [19, 20]. Due to the low carrier concentration in PZT the contact properties define whether majority electronic carriers in PZT are either electrons or holes. The interface formation between PZT and e.g. Pt was studied using photoelectron spectroscopy [21, 22, 23, 24]. Scott *et al.* have used a device model to derive the Fermi level position at the interface of $E_F - E_{VB} = 1.6$ eV using PZT electron affinity and metal work function [1, 25]. For the PZT/Pt interface we have recently reported a Fermi level position $E_F - E_{VB} = 1.6 \pm 0.1$ eV after Pt deposition, directly derived using *in-situ* photoelectron spectroscopy. However, the barrier height is depending on the chemical state of the interface. After Pt deposition a reduced PZT/Pt interface was found, as could be derived from the occurrence of metallic Pb in the Pb 4f X-ray induced photoelectron spectra of PZT. After an annealing step in O_2 the interface was oxidized and a Fermi level position $E_F - E_{VB} = 1.1 \pm 0.1$ eV was found,

while after two weeks in ultra high vacuum at room temperature a strong reduction of the PZT/Pt interface and a Fermi level position 2.2 ± 0.1 eV above the VBM was observed [24]. Taking the band gap of PZT of 3.4 eV [1] into account, this amounts to a Schottky barrier height for holes of 1.1 ± 0.1 eV for the oxidized and a Schottky barrier height for electrons of 1.2 ± 0.1 eV for the reduced PZT/Pt interface. Accordingly, in dependence on the interface state a preference for hole or electron injection is possible at the PZT/Pt interface.

Takatani *et al.* have also found a shift of the Fermi level towards lower $E_F - E_{VB}$ upon annealing in O_2 but did not give absolute values for the Schottky barrier heights [21, 22]. For the $SrTiO_3/Pt$ and SnO_2/Pt interfaces a variation of the Schottky barrier of up to 1 eV, depending on preparation conditions, has also been reported [26, 27]. The studied Oxide/Pt interfaces are therefore chemically unstable and are readily oxidized or reduced depending on the preparation and post-deposition treatment conditions [26].

In order to investigate the interface properties between PZT and oxidic electrodes, RuO_2 and ITO were chosen as material candidates with strongly different work functions. RuO_2 is an oxide showing metallic conductivity [28] while ITO is a degenerately doped semiconductor [29]. The former has a high work function of ~ 6.1 eV [30] while highly doped as-deposited ITO films have a work function of ~ 4.5 eV [31, 32]. In this work the interface formation between PZT and RuO_2 as well as PZT and ITO were studied *in-situ* using photoelectron spectroscopy. It is shown that the barrier height between PZT and the two studied oxides differs significantly and the electronic transport mechanism in PZT is changed from a preference for hole injection for RuO_2 to a preference for electron injection for ITO.

2. Experimental

The experiments were performed at the DArmstadt Integrated SYstem for MATerial research (DAISY-MAT), which combines a Physical Electronics PHI 5700 multitechnique surface analysis system with several deposition chambers via an ultrahigh vacuum sample transfer [33]. X-ray photoelectron spectra were recorded using monochromated Al $K\alpha$ radiation with an overall energy resolution of ~ 0.4 eV, as determined from the Gaussian broadening of the Fermi edge of a sputter cleaned Ag sample. Binding energies are given with respect to the Fermi level of a sputter cleaned Ag sample with an accuracy of ~ 50 meV. All spectra were recorded using a takeoff angle of 45° .

Polycrystalline PZT thin films were prepared at the Hefei National Laboratory for Physical Sciences at the Microscale of the University of Science and Technology of China by pulsed laser deposition using a KrF 248 nm excimer laser with a repetition rate of 10 Hz and an energy density of 1.8 J/cm². The PZT target with a Zr/Ti ratio close to the morphotropic composition (52/48) was made by standard solid state reaction. The distance between the substrate and target during deposition was 5 cm, the substrate temperature 650°C and the oxygen pressure 30 Pa. Using these parameters, the growth

rate for PZT is ~ 15 nm/min. The PZT thin films were deposited on commercially available platinized Si wafers from Inostek. For the interface formation with ITO a PZT film of 200 nm thickness was used while for the interface formation with RuO_2 a 50 nm thick PZT film was utilized.

ITO and RuO_2 were deposited in one of the deposition chambers of the DAISY-MAT system. ITO was deposited by radio frequency magnetron sputtering from a ceramic target, being composed of 90 wt% In_2O_3 and 10 wt% SnO_2 . A power density of 1.25 W/cm², a substrate temperature of 400 °C, a pressure of 0.5 Pa, a substrate to target distance of 9 cm, and pure Ar as sputter gas were utilized. With these conditions highly doped ITO films with an electrical resistivity of $\sim 2 \cdot 10^{-4}$ Ω cm and a work function of ~ 4.5 eV are obtained [31]. RuO_2 was deposited by reactive direct current magnetron sputtering from a metallic Ru target with a power density of 0.5 W/cm². The substrates were held at room temperature during deposition. A pressure of 1 Pa, a substrate to target distance of 10 cm, and an Ar/O₂ ratio of $92.5/7.5$ were used. The deposition conditions were chosen to guarantee the formation of fully oxidized RuO_2 , as verified by photoelectron spectroscopy as reported previously [30].

3. Results and Discussion

3.1. Survey spectra

Figure 1 shows X-ray induced survey spectra of a PZT thin film sample after surface cleaning via heating in O₂ as well as of the ~ 10 nm thick RuO_2 and ITO thin films deposited during the interface experiments. In the case of the PZT thin film only emissions from Pb, Zr, Ti, and O are present. A C 1s emission due to adsorbed hydrocarbons lying at a binding energy of $E_B \sim 285$ eV can not be found, showing that the PZT film surfaces are free of contaminations. Also in the course of RuO_2 as well as of ITO deposition there is no carbon present. In the RuO_2 (ITO) survey spectra only emissions of the elements Ru and O (In, Sn and O) are found. In the case of the RuO_2 the Ru 3d doublet, while lying in the vicinity of the C 1s emission, completely describes the measured spectrum at ~ 280 - 290 eV binding energy (see also Fig. 2).

3.2. Deposition of RuO_2 on PZT

X-ray induced photoelectron core level spectra of the PZT thin film recorded in the course of RuO_2 deposition are shown in Fig. 2. During the stepwise deposition of RuO_2 the substrate cation intensities decrease and the Ru emission increases until a RuO_2 thickness of ~ 10 nm is reached and the PZT cation emissions are almost completely attenuated. All substrate cation emissions decay exponentially with decay constants corresponding to the inelastic mean free path of the individual lines, indicating a layer-by-layer growth mode. The shape of the PZT cation emission does not change with increasing RuO_2 thickness except for the Ti spectrum, where the Ru $3p_{3/2}$ emission is superimposed with the Ti $2p_{1/2}$ emission at a binding energy of ~ 464 eV. The change

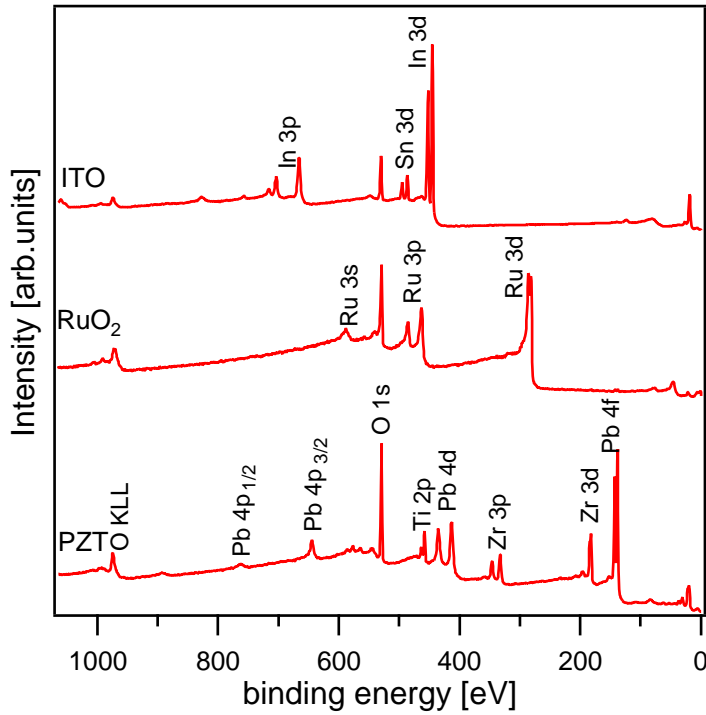


Figure 1. X-ray photoelectron survey spectra of a PZT thin film after surface cleaning and of *in-situ* deposited RuO_2 and ITO thin films.

of lineshape of the O 1s emission can be explained by the shift from insulating PZT, having a symmetric emission, to metallic RuO_2 with an asymmetric Doniach-Sunjić profile [34]. All cation emissions from PZT exhibit a parallel shift of ~ 0.8 eV to lower binding energies in the course of deposition. From the unchanged substrate cation emission lineshapes as well as from their parallel shift in the course of RuO_2 deposition an interface reaction between PZT and RuO_2 can be ruled out. At small RuO_2 coverages the Ru $3d_{3/2}$ emission lies at considerable lower binding energies than expected for RuO_2 (binding energy of ~ 281 eV) while reaching the known value for higher RuO_2 thickness. Such a behavior is frequently observed in this kind of experiments and is typically explained by incomplete screening of the core hole in small metal islands occurring in the initial growth state [35].

3.3. Schottky barrier at the PZT/ RuO_2 interface

The Schottky barrier is determined by the position of the Fermi level in the PZT at the interface. In the inset of Fig. 3 the valence band spectra of the uncovered PZT film as well as of the 10 nm thick RuO_2 film, grown on the PZT substrate, are shown. The valence band maximum (VBM) of PZT is determined from the linear extrapolation of the leading edge of the valence band spectrum with an uncertainty of ± 0.1 eV. The valence band maximum of the PZT sample lies at 1.7 ± 0.1 eV. In Fig. 3 the evolution of the substrate core level lines during stepwise deposition of RuO_2 are shown. For better

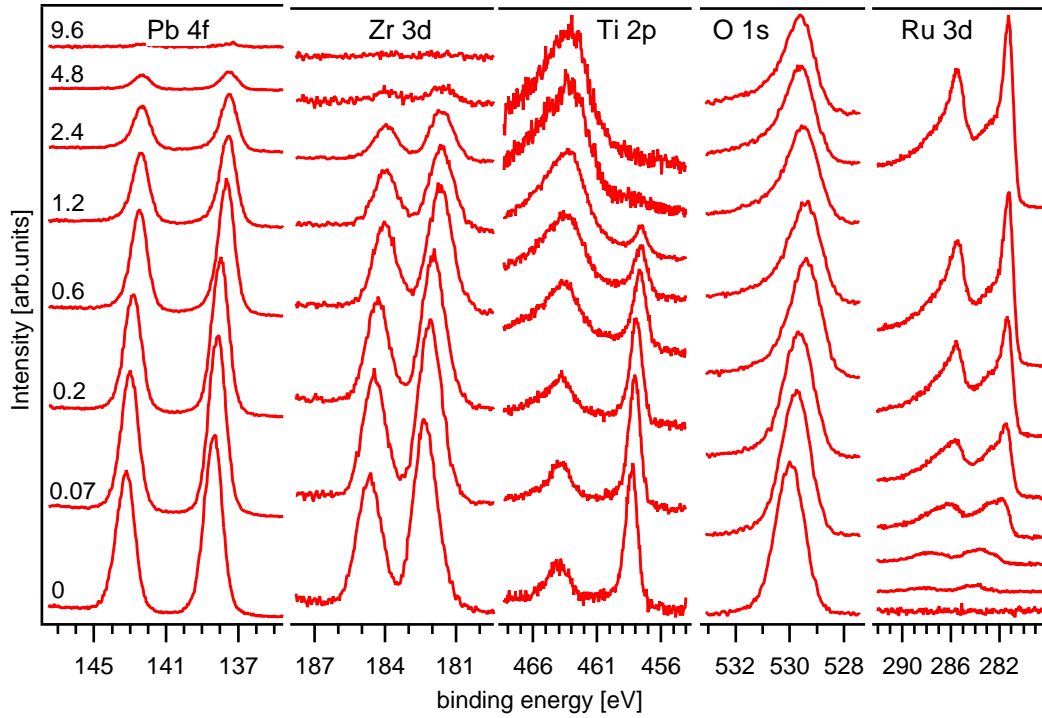


Figure 2. X-ray photoelectron core level spectra of the PZT sample recorded in the course of RuO_2 deposition. The RuO_2 thickness is given in nm.

comparison the difference between core level binding energies and valence band maxima, as obtained from the uncoated substrate, were subtracted. The shifts of the core level binding energies saturate at $E_F - E_{VB} = 1.0 \pm 0.1$ eV for RuO_2 thickness > 1 nm. The Schottky barrier height for holes $\Phi_{B,h}$ can therefore directly be extracted, amounting to 1.0 ± 0.1 eV for the PZT/ RuO_2 interface.

3.4. Deposition of ITO on PZT

In Fig. 4 X-ray photoelectron core level emissions of the PZT film are presented in course of ITO deposition. With increasing ITO thickness the PZT cation core emissions are exponentially attenuated, indicating a layer by layer growth of the ITO film. As observed for the PZT/ RuO_2 interface, no change of the PZT cation lines is visible with increasing ITO thickness. The O 1s emission shows an increasing asymmetry with larger ITO thickness, which is related to Plasmon excitations of the electron gas of the degenerately doped material [31]. For low ITO coverages up to 0.5 nm all PZT core emissions are shifted in parallel by ~ 0.4 eV to higher binding energies. After the first ITO deposition step the In 3d binding energy exhibits a parallel shift. Reaching an ITO thickness of ~ 1 nm all spectra are shifted by ~ 0.5 eV to lower binding energies. The evolution of the binding energies with increasing ITO overlayer thickness will be explained in section 3.5. From the unchanged PZT cation and In lineforms, as well as the parallel shift of the PZT cation lines, an interface reaction between PZT and ITO

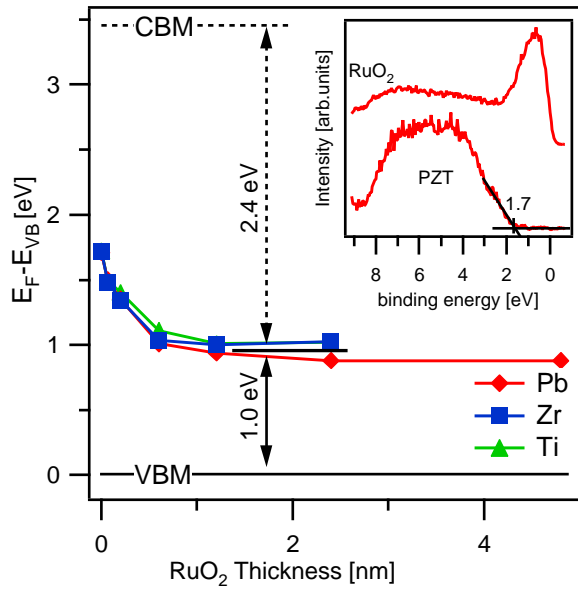


Figure 3. Evolution of the PZT core level lines with increasing RuO_2 thickness. The distance between core level lines and VBM have been subtracted. The Schottky barrier height for holes $\Phi_{B,h}$, corresponding to the distance between Fermi level E_F and valence band maximum position E_{VB} , amounts to 1.0 ± 0.1 eV as determined from the saturation of the core level binding energy shifts. Taking the band gap of PZT of 3.4 eV into account [1], this leads to a Schottky barrier for electrons of 2.4 ± 0.1 eV. VBM and CBM refer to the band edges of PZT. In the inset the X-ray photoelectron valence band spectra of the uncovered PZT film as well as of the 10 nm thick RuO_2 film grown on the PZT substrate are shown.

can be ruled out.

3.5. Band alignment between PZT and ITO

The band alignment between PZT and ITO is determined from the evolution of the PZT and ITO cation emissions with increasing ITO thickness, as presented in Fig. 5. In the inset the valence band spectra of the uncovered PZT sample as well as the 12 nm thick ITO film grown on PZT are shown. The valence band maxima positions are derived from the leading edge of the valence bands and lie at 2.3 ± 0.1 eV and 3.25 ± 0.1 eV for uncoated PZT and thick ITO, respectively. In the ITO valence band spectrum the emission at the low binding energy side of the valence band maximum at ~ 2 -3 eV binding energy can be explained by partially unsaturated cations ([31] and references within). The 0.6 eV higher VBM position of the 200 nm thick uncoated PZT film used for the PZT/ITO interface study, as compared to the 50 nm thick PZT film used for the PZT/ RuO_2 interface, indicates a slight charging of the PZT. Due to the parallel shift of substrate and overlayer binding energies, the band alignment can be reliably determined from the difference of the valence band maxima of PZT and ITO, which are derived from the respective core level binding energies. The discontinuous evolution

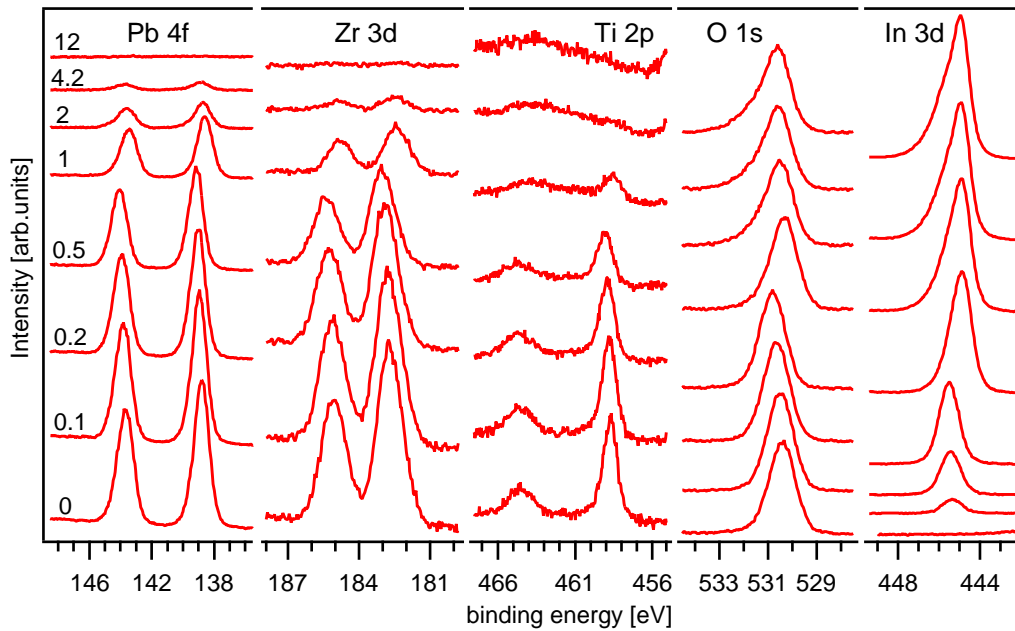


Figure 4. X-ray photoelectron core level spectra of the PZT sample in the course of ITO deposition. The ITO thickness is given in nm.

of binding energies between 0.5 and 1 nm ITO thickness is explained by compensation of the charging effect: Once the thickness of ITO exceeds a certain limit, it becomes conductive enough to short-circuit the sample surface with the electrically grounded sample holder [36]. The compensation of the charging effect is verified by the valence band maximum binding energy of the thick ITO film, which is within the range expected for comparably prepared films [31]. This guarantees that the barrier height for charge injection, which is given by the Fermi level position at the interface, is not affected by charging and can thus directly be derived from Fig. 5.

As presented in Fig. 5 a Fermi level position at the PZT/ITO interface of $E_F - E_{VB} = 2.1 \pm 0.2$ eV is deduced for ITO thickness ≥ 1 nm. The Fermi level at the PZT/ITO interface is thus in the upper half of the band gap. Since the PZT core level lines do not completely saturate at larger ITO thickness, a higher margin of error is assumed. Taking the band gap of PZT of 3.4 eV [1] into account, this results in a Schottky barrier for electrons of 1.3 ± 0.2 eV. Furthermore, a valence band offset between PZT and ITO of 1.1 ± 0.1 eV is derived with the ITO VBM lying at lower binding energies.

3.6. Comparison of barrier heights

The difference of the Fermi level position at the contact between PZT and RuO_2 or ITO of 1.1 eV is almost as large as the difference in work function of RuO_2 and ITO of 1.6 eV. This points to a less strong Fermi level pinning for PZT with oxide electrodes than calculated by Robertson and Chen using charge neutrality levels (CNL) [39]. They

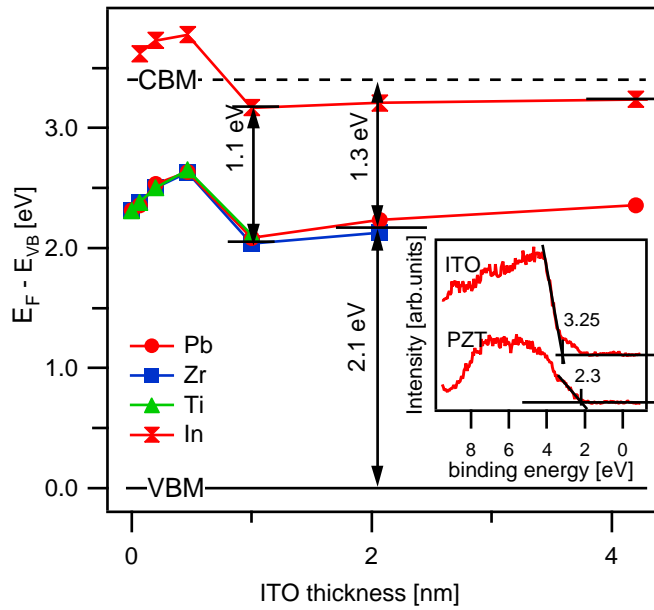


Figure 5. Evolution of the PZT core level lines with increasing ITO thickness d_{ITO} . The distance between core level lines and VBM has been subtracted. From the Fermi level position ~ 2.1 eV above the valence band maximum a Schottky barrier for electrons of ~ 1.3 eV can be derived, using a band gap of 3.4 eV for PZT. In addition the valence band offset between PZT and ITO of ~ 1.1 eV can be deduced from the graph. VBM and CBM refer to the band edges of PZT. In the inset the X-ray photoelectron valence band spectra of the uncovered PZT film as well as of the 12 nm thick ITO film grown on the PZT substrate are shown.

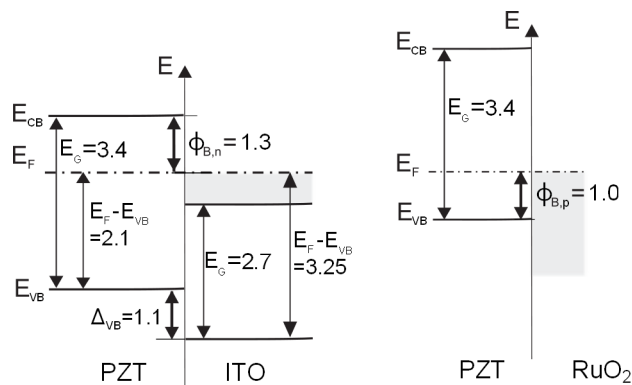


Figure 6. Schematic band diagram of the PZT/ITO contact (left) and the PZT/ RuO_2 contact (right). ITO is a degeneratively doped semiconductor having a fundamental band gap of ~ 2.7 eV [37, 38] with the Fermi level lying in the conduction band, as also confirmed by the valence band maxima position of 3.25 eV. All energies given in electron Volt.

have derived a pinning index of 0.31 for $PbTiO_3$ and 0.4 for $PbZrO_3$, which gives ~ 0.4 - 0.64 eV difference in barrier height for RuO_2 and ITO. This is considerably less than the experimentally found value of 1.1 eV. It is also astonishing that the Fermi level at the contact between RuO_2 and PZT is found just 1 eV above the valence band maximum. In the case of the $(Ba, Sr)TiO_3/RuO_2$ interface the Fermi level lies ~ 2.3 eV above the VBM [30]. The charge neutrality levels for $SrTiO_3$ and $PbZrO_3$ calculated by Robertson are both at 2.6 eV above the VBM, while the CNL for $PbTiO_3$ is calculated to lie at 1.9 eV [40]. For an almost equal mixture of $PbTiO_3$ and $PbZrO_3$, as used for this study, a higher Fermi level position would have been expected at the PZT/ RuO_2 interface from theory.

4. Summary and Conclusions

We have investigated the interface formation between PZT and RuO_2 and ITO, respectively using *in-situ* photoelectron spectroscopy. Stepwise deposition of RuO_2 and ITO were performed via magnetron sputtering on contamination free PZT thin films, being prepared beforehand by PLD on platinized Si wafers. Both studied interfaces are not reactive in contrast to the PZT/Pt interface, where a reduction of PZT is observed upon deposition of Pt [21, 22, 24]. A schematic energy band diagram of the deposited PZT/ITO, together with the PZT/ RuO_2 contact, are given in Fig. 6. In case of the PZT/ RuO_2 interface a Schottky barrier for holes of 1.0 ± 0.1 eV was found. For the PZT/ITO interface a Schottky barrier for electrons of 1.3 ± 0.2 eV was derived. This shows that using different oxide electrode materials allows for engineering of the contact properties. For PZT a transition from preference for hole injection to a preference for electron injection can be achieved when switching from RuO_2 to ITO electrodes.

Acknowledgement

The work was supported by the German Science Foundation within the collaborative research center SFB 595 (Electrical Fatigue of Functional Materials).

References

- [1] J. F. Scott, *Ferroelectric memories*, Springer Verlag, Heidelberg, 2000.
- [2] A. J. Moulson and J. M. Herbert, *Electroceramics: Materials, Properties, Applications (2nd edition)*, John Wiley and Sons, New York, 2003.
- [3] A. K. Tagantsev, I. Stolichnov, E. L. Colla, and N. Setter, *Journal of Applied Physics*, 2001, **90**, 1387–1402.
- [4] D. Lupascu and J. Rödel, *Advanced Engineering Materials*, 2005, **7**, 882–898.
- [5] S. D. Bernstein, T. Y. Wong, Y. Kisler, and R. W. Tustison, *Journal of Materials Research*, 1993, **8**(1), 12–13.
- [6] D. J. Lichtenwalner, R. Dat, O. Auciello, and A. I. Kingon, *Ferroelectrics*, 1994, **152**, 97–102.
- [7] C. B. Eom, R. B. Van Dover, J. M. Phillips, D. J. Werder, J. H. Marshall, C. H. Chen, R. J. Cava, R. M. Fleming, and D. K. Fork, *Applied Physics Letters*, 1993, **63**(18), 2570–2572.

- [8] P. J. Schorn, D. Bräuhäus, U. Böttger, R. Waser, G. Beitel, N. Nagel, and R. Bruchhaus, *Journal of Applied Physics*, 2006, **99**, 114104.
- [9] J. F. M. Cillessen, M. W. J. Prins, and R. M. Wolf, *Journal of Applied Physics*, 1997, **81**(6), 2777–2783.
- [10] J. J. Lee, C. L. Thio, and S. B. Desu, *Journal of Applied Physics*, 1995, **78**(8), 5073–5078.
- [11] C. M. Foster, R. Csencsits, G. R. Bai, Z. Li, L. A. Wills, R. Hiskes, H. N. Al-Shareef, and D. Dimos, *Integrated Ferroelectrics*, 1995, **10**, 31 – 38.
- [12] A. V. Rao, S. A. Mansour, and A. L. Bement, *Materials Letters*, 1996, **29**, 255–258.
- [13] L. Pintilie, I. Vrejoiu, D. Hesse, and M. Alexe, *Applied Physics Letters*, 2006, **88**(10), 102908–3.
- [14] F. Chen, Q. Z. Liu, H. F. Wang, F. H. Zhang, and W. Wu, *Applied Physics Letters*, 2007, **90**(19), 192907–3.
- [15] X. Du and I. W. Chen, *Journal of Applied Physics*, 1998, **83**(12), 7789–7798.
- [16] R. Gerson and H. Jaffe, *Journal of Physics and Chemistry of Solids*, 1963, **24**(8), 979–984.
- [17] L. Wu, T. S. Wu, C. C. Wei, and H. C. Liu, *Journal of Physics C: Solid State Physics*, 1983, **16**(14), 2823.
- [18] D. J. Wouters, G. J. Willems, and H. E. Maes, *Microelectronic Engineering*, 1995, **29**(1-4), 249–256.
- [19] S. M. Sze and K. K. Ng, *Physics of Semiconductor Devices, 3rd edition*, John Wiley and Sons, New York, 2006.
- [20] W. Mönch, *Semiconductor Surfaces and Interfaces*, Springer Verlag, Heidelberg, 1993.
- [21] S. Takatani, K. Kushida-Abdelghafar, and H. Miki, *Japanese Journal of Applied Physics, Part 2-Letters*, 1997, **36**(4A), L435–L438.
- [22] S. Takatani, H. Miki, K. Kushida-Abdelghafar, and K. Torii, *Journal of Applied Physics*, 1999, **85**(11), 7784–7791.
- [23] M. Kurasawa and P. C. McIntyre, *Journal of Applied Physics*, 2005, **97**, 104110.
- [24] F. Chen, R. Schafraneck, W. Wu, and A. Klein, *Journal of Physics D: Applied Physics*, 2009, **42**, 215302.
- [25] J. Scott, K. Watanabe, A. Hartmann, and R. Lamb, *Ferroelectrics*, 1999, **225**, 83–90.
- [26] R. Schafraneck, S. Payan, M. Maglione, and A. Klein, *Physical Review B*, 2008, **77**, 195310.
- [27] C. Körber, S. P. Harvey, T. O. Mason, and A. Klein, *Surface Science*, 2008, **602**, 3246–3252.
- [28] J. Riga, N. Tenret, C. l, J. J. Pireaux, R. Caudano, J. J. Verbist, and Y. Gobillon, *Physica Scripta*, 1977, **16**(5-6), 351–354.
- [29] I. Hamberg and C. Granqvist, *Journal of Applied Physics*, 1986, **60**, R123.
- [30] R. Schafraneck, J. Schaffner, and A. Klein, *Journal of the European Ceramic Society*, 2010, **30**, 187–192.
- [31] Y. Gassenbauer, R. Schafraneck, A. Klein, S. Zafeiratos, M. Havecker, A. Knop-Gericke, and R. Schlögl, *Physical Review B*, 2006, **73**, 245312.
- [32] A. Klein, C. Körber, A. Wachau, F. Säuberlich, Y. Gassenbauer, R. Schafraneck, S. P. Harvey, and T. O. Mason, *Thin Solid Films*, 2009, **518**, 1197–1203.
- [33] D. Ensling, A. Thißen, Y. Gassenbauer, A. Klein, and W. Jaegermann, *Advanced Engineering Materials*, 2005, **7**, 945–949.
- [34] S. Doniach and M. Sunjic, *Journal of Physics C*, 1970, **3**, 285–291.
- [35] G. K. Wertheim, *Zeitschrift für Physik D*, 1989, **12**, 319–326.
- [36] A. Klein, Y. Tomm, R. Schlaf, C. Pettenkofer, W. Jaegermann, M. Lux-Steiner and E. Bucher, *Solar Energy Materials and Solar Cells*, 1998, **51**, 181–191.
- [37] A. Bourlange, D. Payne, R. Egdell, J. Foord, P. Edwards, M. Jones, A. Schertel, P. Dobson, and J. Hutchison, *Applied Physics Letters*, 2008, **92**, 092117.
- [38] A. Walsh, J. L. F. Da Silva, S.-H. Wei, C. Körber, A. Klein, L. F. J. Piper, A. DeMasi, K. E. Smith, G. Panaccione, P. Torelli, D. J. Payne, A. Bourlange, and R. G. Egdell, *Physical Review Letters*, 2008, **100**, 167402.
- [39] J. Robertson and C. W. Chen, *Applied Physics Letters*, 1999, **74**(8), 1168–1170.

[40] J. Robertson, *Journal of Vacuum Science and Technology B*, 2000, **18**(3), 1785–1791.